18th International Conference on Information Fusion
Washington, DC - July 6-9, 2015

Direct Single Sensor TDOA Localization Using Signal Structure Information

Christian Steffes and Marc Oispuu
Fraunhofer FKIE, Wachtberg, Germany
Dept. Sensor Data and Information Fusion
{christian.steffes, marc.oispuu}@fkie.fraunhofer.de

***Abstract*—In this paper, a new single sensor passive emitter localization approach is presented. The use of signal structure information allows TDOA-based localization with a single moving sensor node. A direct position estimation scheme is derived for the single sensor TDOA localization problem. The feasibility of the proposed method is shown in simulations. The position estimation accuracy of the single senor TDOA and the direct technique are compared. Field experiments using an airborne sensor are conducted to prove the concept.**

I. Introduction

Passive emitter localization is a fundamental task encountered in various fields like wireless communication, radar, sonar, seismology, and radio astronomy. An airborne sensor platform is the preferable solution in many applications. The sensor is typically mounted e.g. on an aircraft, a helicopter, or an unmanned aerial vehicle (UAV). Airborne sensors provide in comparison to ground located sensors a far-ranging signal acquisition because of the extended radio horizon. Mostly for localization issues, sensors are installed under the fuselage or in the wings of the airborne sensor platform. In case of hard payload restrictions only compact sensors come into consideration.

Aspects of the two-dimensional and three-dimensional localization problem examined in the literature include numerous estimation algorithms, estimation accuracy, and target observability [2]. Typical localization systems of interest obtain measurements like direction of arrival (DOA), frequency difference of arrival (FDOA), time difference of arrival (TDOA) or combinations of the aforementioned measurements [3].

Commonly, the desired source locations are determined in multiple steps: the signal processing step where the sensor data is computed from the raw signal data, and the sensor data fusion step where the localization and tracking task is performed. Alternatively, direct position determination (DPD) approaches have been proposed to compute the desired target parameters in a single step based on the raw signal data without explicitly computing intermediate measurements like DOA, FDOA, and TDOA [12], [11]. It has been shown that this kind of data processing offers a superior performance in scenarios with weak or closely-spaced sources but requires a higher computational burden in comparison to the standard multi-step processing. For example for TDOA-based localization, a direct approach based on the raw signal data has been proposed in [12], [1], and a standard approach based on TDOA/FDOA measurements has been proposed in [9], [10], respectively. In [6], a localization approach based on the complex ambiguity function (CAF) has been introduced which turned out to be a compromise between localization performance and computational burden.

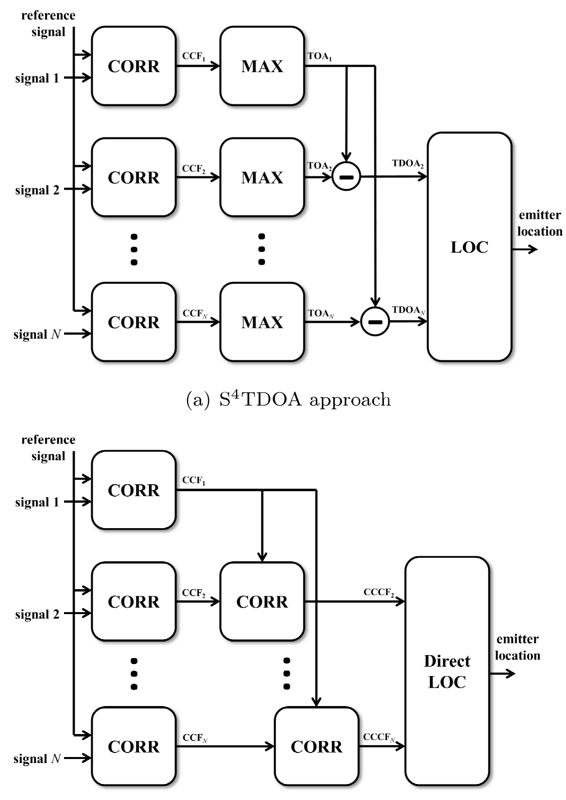

(a) S^{4}TDOA approach

(b) DS^{4}TDOA

Figure 1. Comparison of non-direct and direct approach.

In our previous work, we proposed a DPD approach for a moving antenna array sensor [5], [4]. Furthermore in [8], we introduced a *single element* TDOA localization approach using just a single omnidirectional antenna. In the following, this approach is referred to as single sensor signal structure TDOA (S^4TDOA) localization (Fig. 1(a)). Commonly, single-element approaches using a single directional antenna take the directions in which local maximum power is received to be the DOA estimates [7]. Since directional antennas cannot simultaneously scan in all directions, some transient signals can escape detection and fluctuations of the source signal strength and polarization during the sequential lobing process may have a significant impact on the DOA accuracy. However, these problems are circumvented by the technique proposed in [8] which is applicable when information about the signal structure is a priori known (e.g. communication and radar emitters).

In this paper, the single-element TDOA localization approach is extended by the key-idea of direct emitter localization. For an airborne scenario with a single stationary source, we introduce a novel direct localization approach based on the cross correlation function (CCF). Our simulation and experimental measurement results demonstrate that the proposed approach considerably outperforms the standard single-element localization approach. This approach is named as direct S^4TDOA abbreviated with DS^4TDOA (Fig. 1(b)).

This paper is organized as follows: In Section II, the considered localization problem is stated. In Section III, we briefly review the S^4TDOA localization approach based on the CAF [8] and introduce the novel DS^4TDOA approach. Simulation results comparing both approaches are presented in Section IV. In Section V, the experimental measurement results proof the concept. Finally, the conclusions are given in Section VI.

The following notations are used throughout this paper: $f[k]$ is a discrete version of the function $f(t)$, $f^*[k]$ is the conjugate complex of the function $f[k]$, and $(\cdot)^T$ denotes transpose.

II. Problem Formulation

We consider an omnidirectional antenna sensor mounted on an airborne platform moving along an arbitrary but known sensor path observing a single ground-located source at position $\mathbf{x}$. The source emits a continuous signal with a known periodic pulse structure given by

$$s(t) = \sum_{i=-\infty}^{+\infty} \sqcap(t - iT)\,, \tag{1}$$

where $\sqcap(\cdot)$ denotes a rectangular function with some pulse width T_p and $T > T_\mathrm{p}$ denotes the pulse repetition interval. E.g. in case of a communication signal, the pulse structure represents the transmission and guard intervals of the signal.

During the movement, the sensor collects N signal data batches. The n-th received signal at some measurement point reads

$$z_n(t) = a_n\, s(t - t_{\mathrm{e},n} - t_n)\, \exp(\mathrm{j}\,\nu_n t) + w_n(t)\,, \tag{2}$$

where a_n denotes a path attenuation factor, $t_{\mathrm{e},n}$ denotes the unknown signal emission time of the n-th received signal, t_n denotes the time difference between signal emission and signal acquisition, ν_n is the signal Doppler shift induced by the movement of the own sensor platform, and w_n denotes some addtional receiver noise,$n = 1, ..., N$.

In practice, the sensor collects data samples from the received signal. In the considered scenario, the sampling rate is assumed to be high enough that the sensor location $\mathbf{r}_n$ is approximately constant for each collected data batch (Fig. 2). Then, t_n and ν_n are given by

$$t_n(\mathbf{x}) = \frac{||\triangle \mathbf{r}_n(\mathbf{x})||}{c}\,, \tag{3}$$

$$\nu_n(\mathbf{x}) = \frac{\mathbf{v}_n^T \triangle \mathbf{r}_n(\mathbf{x})}{||\triangle \mathbf{r}_n(\mathbf{x})||}\,\frac{f_0}{c}\,, \tag{4}$$

respectively, where $\triangle \mathbf{r}_n(\mathbf{x}) = \mathbf{x} - \mathbf{r}_n$ denotes the relative vector between sensor and source, $\mathbf{v}_n$ is the sensor velocity vector, c is the signal propagation speed, and f_0 is the center frequency of the emitted signal.

Considering the time-discrete version of the received signal in (2), the k-th data sample of the n-th data batch is given by

$$z_n[k] = a_n\, \tilde{s}[k\triangle - \mathrm{clk}_n - \tau_n]\, \exp(\mathrm{j}\,\nu_n k\triangle) + w_n[k]\,, \tag{5}$$

where $\triangle$ is the sample interval, clk_n is the known sensor clock of the n-th measurement, τ_n is the signal time of arrival relative to the sensor clock, and $\tilde{s}[k]$ is a reference signal representing the signal $s[k]$. For the ideal case, it can be assumed that $\tilde{s}[k] = s[k]$. Please note that $\mathrm{clk}_n + \tau_n = t_{\mathrm{e},n} + t_n$ holds. The additional receiver noise w_n is assumed to be temporally uncorrelated and zero-mean Gaussian.

Finally, the localization problem is stated as follows: Estimate the source location $\mathbf{x}$ from the received signal data batches $\mathbf{z}_n = (z_n[1], ..., z_n[K])^T$, $n = 1, ..., N$.

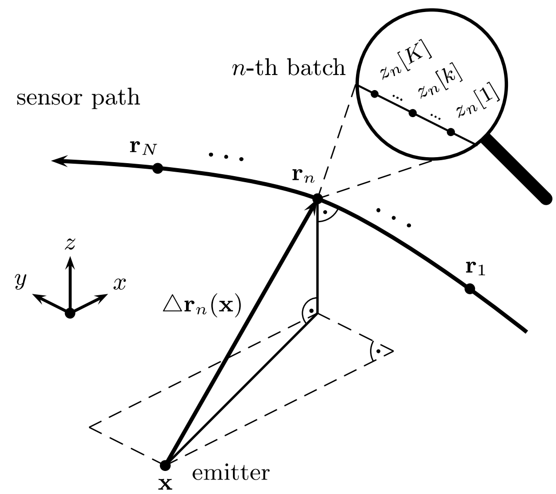

Figure 2. Three-dimensional localization scenario.

III. Localization Approaches

In this section, approaches for the stated localization problem are presented i.e. the localization of a source with periodic pulse emission using a single moving sensor. Firstly, an approach based on TOA measurements is presented. Then, the proposed novel approach based on the CCF is presented. For the sake of simplicity, only TOA measurements are considered in following and the Doppler is neglected. Nevertheless, the following techniques could be generalized to full CAF.

A. Two-step S^4TDOA Approach

Step 1: Commonly for a sensor network, TDOA measurements are extracted from the CCF

$$\mathrm{CCF}(\triangle\tau) = \sum_{k=1}^{K} z_1^*[k] z_2[k+\triangle\tau]\,, \tag{6}$$

i.e. from the correlation of the two signals $z_1[k]$ and $z_2[k]$ in time domain. The TDOA estimates are calculated by detecting the peak in the CAF:

$$\triangle\hat{\tau} = \arg\max_{\triangle\tau} \mathrm{CCF}(\triangle\tau)\,. \tag{7}$$

However, since a single moving sensor is considered, the measurements are not taken simultaneously. Thus in the following, the signal processing for the single sensor case is presented (Fig. 1(a)). Due to the known signal structure, a quasi-TDOA measurement can be computed by considering the individual known sensor clock clk_n:

$$\hat{\tau}_n = \arg\max_{\tau} \mathrm{CCF}_n(\tau) \tag{8}$$

with

$$\mathrm{CCF}_n(\tau) = \sum_{k=1}^{K} z_n^*[k]\tilde{s}[k+\mathrm{clk}_n+\tau]\,, \tag{9}$$

where $\tilde{s}[k]$ denotes a reference signal introduced in (5). Then similar to (7), a quasi-TDOA measurement can be calculated by taking the clock differenes (Fig. 3)

$$\triangle\mathrm{clk}_{n,r} = \left(\left\lceil\frac{\mathrm{clk}_n-\mathrm{clk}_r}{T}\right\rceil - \left\lfloor\frac{\mathrm{clk}_n-\mathrm{clk}_r}{T}\right\rfloor\right) T \tag{10}$$

into account, where the index r indicates some reference time. Then a quasi-TDOA measurement can be extracted from the TOA estimates by

$$\triangle\hat{\tau}_{n,r} = \hat{\tau}_n - (\hat{\tau}_r + \triangle\mathrm{clk}_{n,r})\,, \tag{11}$$

i.e. by the difference of the individual estimated TOAs corrected by the clock difference. The correction of the clock difference is mandatory because the measurements are not taken simultaneously.

Step 2: The emitter localization problem can be solved by searching the emitter location that most likely explains the TDOA measurements calculated in (11). Therefore, the emitter location can be calculated by solving the following least-squares form:

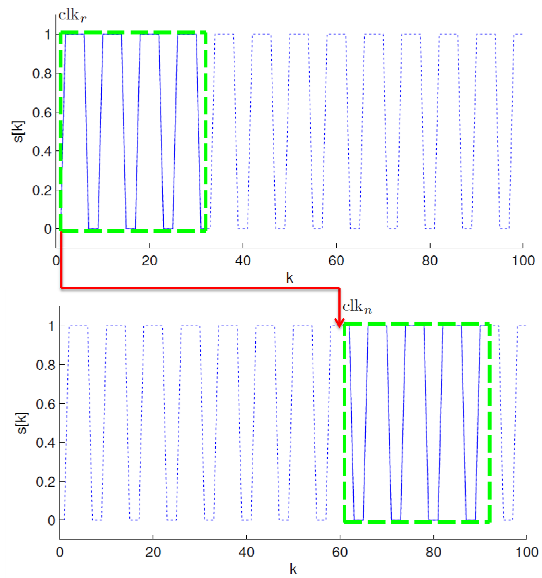

Figure 3. Received signal at measurement step r and n.

$$\hat{\mathbf{x}} = \arg\min_{\mathbf{x}} \sum_{\substack{n=1\\ n\neq r}}^{N} \frac{||\triangle\hat{\tau}_{n,r} - \triangle\tau_{n,r}(\mathbf{x})||^2}{\sigma^2_{\triangle\tau,n,r}}\,, \tag{12}$$

where $\triangle\tau_{n,r}(\mathbf{x})$ denotes the measurement function given analog to (11) by

$$\triangle\tau_{n,r}(\mathbf{x}) = t_n(\mathbf{x}) - (t_r(\mathbf{x}) + \triangle\mathrm{clk}_{n,r})\,, \tag{13}$$

according to (3) and $\sigma^2_{\triangle\tau,n,r}$ denote the TDOA measurement variance, $n = 1, ..., N$. The solution in (12) can be geometrically interpreted as the intersection of the hyperbolae represented by the individual TDOA measurements.

At this point it is worth to mention that in practice, the measurement variances are unknown and vary during the time. Consequently, the measurment variance have to be estimated because otherwise one could use an estimator with a reduced performance.

B. One-step DS^4TDOA Approach

The key-idea of direct localization approaches is to avoid the decision for one TOA/TDOA/AOA measurement in the first step of a localization algorithm. In the case of the S^4TDOA method as described in the previous section, this decision is represented by the process of maximum determination of the CCF. The choice will always falls on the highest peak of the CCF, but when taking into account all measurement batches, this peak might be wrong. In this case, f.e. the second highest peak of the CCF would correspond to the sensor emitter geometry and fit all other measurement batches. Thus, leaving this decision open, allows the implicit evaluation of multiple measurement hypotheses in one localization step.

The intention is to create a cost function that has to be optimized in the localization step, which takes into account all measurement batches at the same time without the explicit decision for TDOAs (Fig. 1(b)). By calculating the CCF of the CCF_r (CCF of $\mathbf{z}_r$ and $s[k]$) and the CCF_n (CCF of $\mathbf{z}_n$ and $s[k]$), the choice for an explicit TDOA can be postponed into the localization step. We call this approach direct single-sensor signal structure TDOA localization (DS^{4}TDOA).

The cost function (cross correlation of cross correlation functions) subject to the position $\mathbf{x}$ is defined as

$$\mathrm{CCCF}_{n,r}(\mathbf{x}) = \sum_{k=1}^{K} \mathrm{CCF}_n^*[k]\mathrm{CCF}_r[k + \triangle\tau_n(\mathbf{x})]\,, \qquad (14)$$

with the CCF given in (9). The localization problem is then stated by

$$\hat{\mathbf{x}} = \arg\max_{\mathbf{x}} \sum_{\substack{n=1\\n\neq r}}^{N} \mathrm{CCCF}_{n,r}(\mathbf{x})\,. \qquad (15)$$

C. Discussion

The localization accuracy for both methods may degrade, if the distance between two observer positions is too big compared to the signal repetition duration T.

If $\triangle\tau_n(\mathbf{x}) \geq \frac{T}{2}$ the wrong peak may be chosen in the maximum determination of the CCFs in the case of S^{4}TDOA. This choice has a direct effect on the localization accuracy using S^{4}TDOA.

The influence on the localization for DS^{4}TDOA is smaller if $\triangle\tau_n(\mathbf{x}) < \frac{T}{2}$ for almost all n. If $\triangle\tau_n(\mathbf{x}) \geq \frac{T}{2}$ for a significant number of measurements , the optimization of the localization function (15) may run into the maximum that corresponds to the wrong time slots. However this is unlikely, because the ambiguities that are due to $\triangle\tau_n(\mathbf{x}) \geq \frac{T}{2}$ are unlike to join in the same spatial position.

IV. Simulation Results

The proposed localization approaches performance is evaluated in Monte-Carlo simulations for a given scenario. GSM base stations are chosen as emitter with recurring signal structure.

A. Simulation Setup

The desired signal is sent on the broadcast channel of a GSM base station and is divided into time slots. Each time slot has a duration of 576.92 μs. A time slot is divided into data transmission time and guard period during which no transmission takes place. This time slot signal structure is represented by the reference signal $\tilde{s}[k]$ introduced in (5).

The sensor trajectory remains the same over all Monte-Carlo runs. The position of the emitter is chosen uniformly at random from a given area of interest. The localization accuracy is also evaluated w.r.t. the signal-to-noise ratio (SNR). A sensor trajectory that is similar to the one of the field experiments (Section V) is used for the simulations. Fig. 4 shows the trajectory as well as the area of interest in which possible emitters are located.

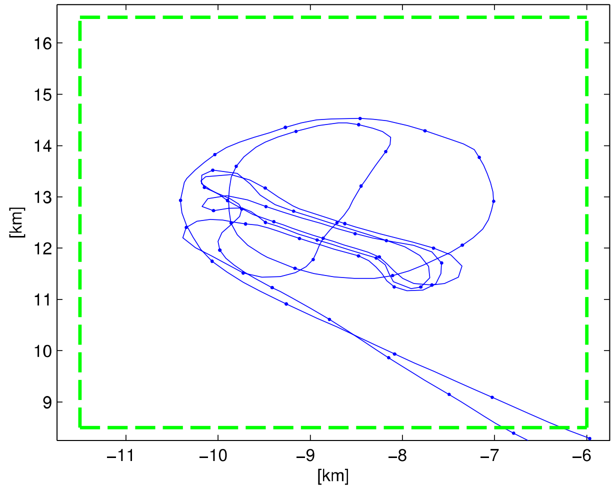

Figure 4. Simulation Scenario: Sensor trajectory and area of interest (green box).

We use the following definition of SNR for the simulations:

$$\mathrm{SNR}_{[\mathrm{dB}]} = 10\log_{10}\frac{\mathrm{P_s}}{\mathrm{P_n}} \qquad (16)$$

with P_s being the mean signal power and P_n the mean noise power. A total of 250 Monte-Carlo runs were performed. Each Monte-Carlo run consists of the following:

1) An emitter position is chosen at random from the area of interest.
2) A random start drift of the broadcast signal is generated.
3) Signal noise for each sensor is generated.
4) For the given observer trajectory and emitter position and time of measurement, corresponding TOAs are calculated.
5) The broadcast signal is embedded into noise in accordance to the respective TOAs and scaled to meet given SNR value.
6) Localization results are calculated using both estimation methods
   a) The initialization is done by evaluating a grid of the respective cost functions for the area of interest.
   b) The position is estimated using Nelder Mead simplex optimization.
7) Points 5 to 6 are repeated for all SNR values in question.

B. Position Estimation

The position estimation for the S^{4}TDOA method is divided into two main steps. In the first step, the received

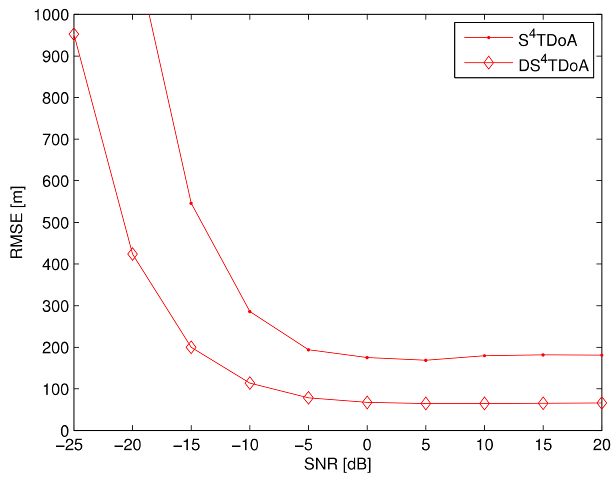

Figure 5. Simulation results: Localization RMSE over SNR for DS^{4}TDOA (red diamonds) and S^{4}TDOA (red dots).

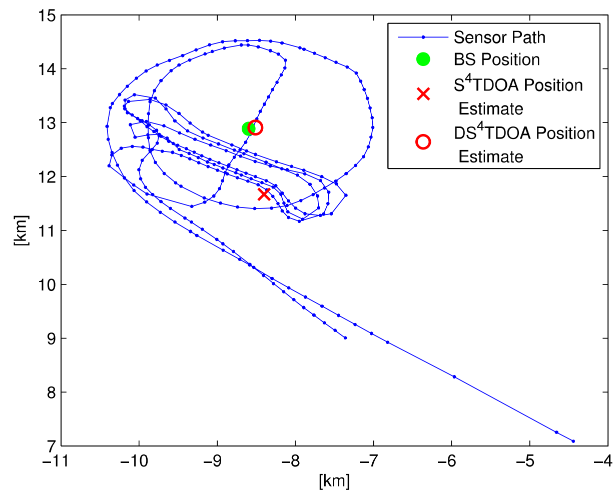

Figure 6. Scenario of field experiments. Sensor trajectory and localization results.

signal is correlated with the stored reference signal. The maximum of this correlation function yields the TOA of each measurement. TOAs of two observation steps form one TDOA measurement. In the second step, the emitter position is estimated based on a set of TDOA measurements.

For the DS^{4}TDOA localization, from the two observation steps that form the TDOA measurement in the above described case, cross correlate the cross correlation functions of the respective received signals and the reference signal. Estimate the emitter position from a set of those cross correlation functions.

For both methods, the respective cost functions are minimized using Nelder/Mead simplex optimization. The initialization problem is solved by evaluating the cost functions of each method for a grid over the area of interest. For the simulations, the grid points were spaced by 100×100 m.

C. Results

Fig. 5 depicts the results of the simulations. For each SNR value, the RMSE of the position estimation over all 250 simulation runs is calculated. The red line with red dots shows the RMSE using the S^{4}TDOA, DS^{4}TDOA is plotted using red diamonds. The accuracy of the DS^{4}TDOA localization approach outperforms the S^{4}TDOA localization method.

V. Experimental Results

Field experiments were conducted to verify the presented method for real data. A GPS time-synchronized sensor node was used to gather data from a GSM mobile station. The sensors receiving antenna was mounted under the wing of an aircraft. The sensor itself and a PC for data processing were installed inside the aircraft. Every five seconds, data from the broadcast channel of the GSM base station was recorded at a sample rate of $f_s = 1$ MHz.

Along with the signal data, corresponding timestamps and position information from the GPS receiver of the sensor are recorded. For each observation time step n, the received signals are filtered and the CCF is calculated. From this CCF the TOA $\hat{\tau}_n$ of the signal is estimated as described in Section III. The CCF, the estimated TOA, the sensors position and time are used in the localization step. The localization estimates for both methods are calculated using the same initialization for the optimization algorithm.

Fig. 6 depicts the sensors trajectory, the position of the GSM base station as well as the localization results using the presented S^{4}TDOA and DS^{4}TDOA method. The presented localization approach is evaluated for different levels of signal strength. Here, a threshold P_t is applied to the measurements. If the mean received signal strength $P_{z_n[k]}$ is below the threshold, the measurement is not used in the localization step. The mean signal strength of a signal $z_n[k]$ is defined as

$$P_{z_n[k]} = \frac{z_n^*[k] z_n[k]}{K} \tag{17}$$

with K being the total number of samples.

Fig. 7 to Fig. 10 show the localization cost functions evaluated for a grid of possible emitter positions. The black line indicates the flight trajectory where the black dots indicate the measurements that are taken into account in the localization step according to the received signal strength threshold. The true position of the emitter is marked by a green dot. The position estimate of the S^{4}TDOA method is shown by a yellow x, the respective DS^{4}TDOA estimate by a red circle.

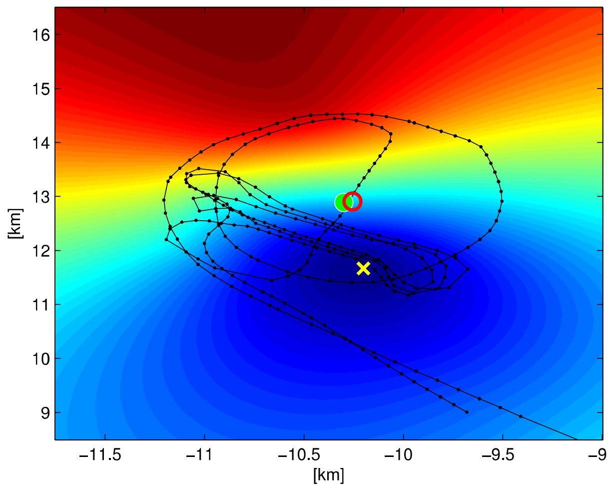

Figure 7. Cost function for S^4TDOA (signal threshold -74 dBm).

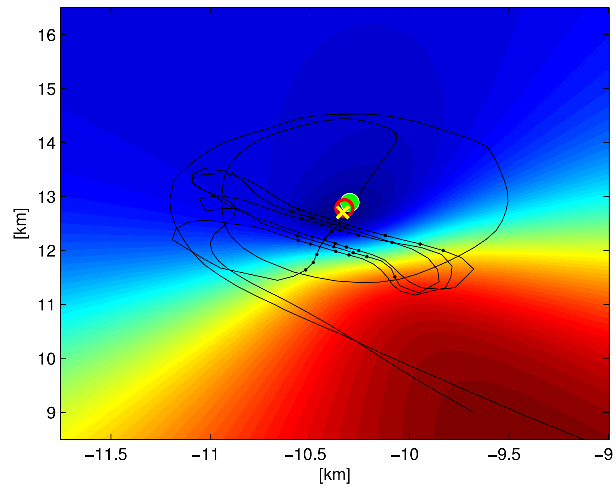

Figure 9. Cost function for S^4TDOA (signal threshold -60 dBm).

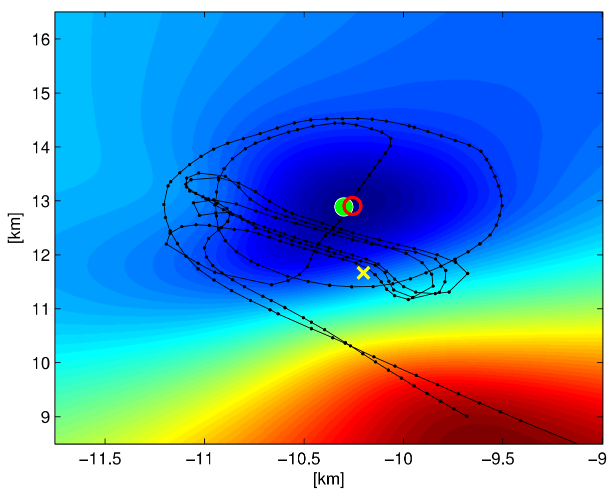

Figure 8. Cost function for DS^4TDOA (signal threshold -74 dBm).

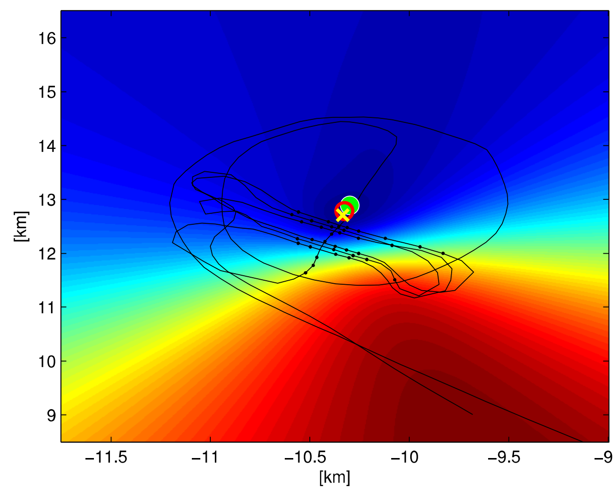

Figure 10. Cost function for DS^4TDOA (signal threshold -60 dBm).

As can be seen in Fig. 7, the minimum of the cost function of the S^4TDOA for a received signal strength threshold level of $P_t = -74\,\mathrm{dBm}$ is not located at the true emitter position due to the choice of one or more faulty TOA values (maximum peaks of the CCF). This results in a larger localization error. Here, the advantage of the DS^4TDOA approach can be seen. Fig. 8 depicts the cost function of the DS^4TDOA method for the same scenario. As can be observed, the minimum of the cost function is located near the true emitter position and the localization result is more accurate. For this scenario with a received signal strength threshold of $P_t = -74\,\mathrm{dBm}$, the 3-D localization error of the S^4TDOA is 1272 m. Using the DS^4TDOA localization algorithm, the position estimation error is 89 m.

The cost function of the S^4TDOA and a received signal strength threshold of $P_t = -60\,\mathrm{dBm}$ is shown in Fig. 9. Less measurements are used to localize the emitter, but due to the higher signal level, the choice of the peak of the CCF as TOA value tends towards the correct peak. With more accurate TDOA estimation, the localization result becomes more accurate. The cost function using the direct localization method (Fig. 10) is very similar to the afore mentioned, also the localization results are nearly the same.

The localization accuracy for the S^4TDOA improves from 1272 m ($P_t = -74\,\mathrm{dBm}$) to 199 m ($P_t = -60\,\mathrm{dBm}$). For the DS^4TDOA location estimation method, a slight

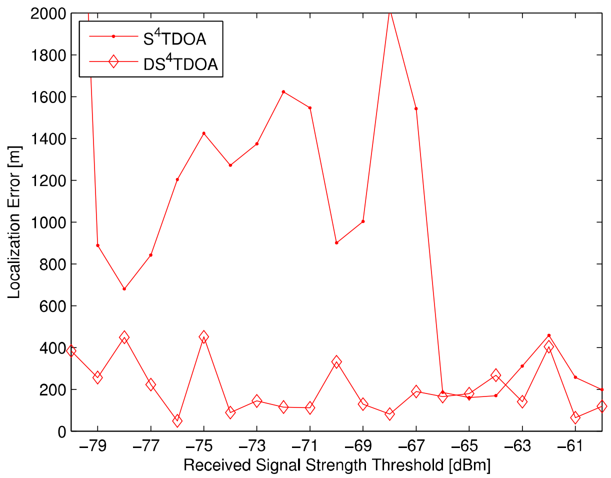

Figure 11. Localization accuracy for different received signal strength thresholds of field experiment data.

degradation of accuracy from 89 m ($P_\mathrm{t} = -74$ dBm) to 119 m ($P_\mathrm{t} = -60$ dBm) is noticed.

Fig. 11 shows the comparison of the localization errors of both methods over different signal strength levels. It can be observed, that the DS^{4}TDOA method is more robust to smaller received signal strength and outperforms the S^{4}TDOA-based method. As the TOA estimation using the signal structure information relies on the amplitude of the signal, with lower SNR, the TOA estimation becomes more and more noisy up until peaks that do not correspond to the signal are chosen as TOA. Since the DS^{4}TDOA method does not require choosing one peak of the CCF, the localization results remain more stable for lower signal level values.

VI. Conclusion

We introduced a direct localization approach for the use with a single moving sensor. The method is based on the S^{4}TDOA found in [8]. The direct localization solution DS^{4}TDOA is derived in Section III. The performance in means of emitter localization accuracy of S^{4}TDOA and DS^{4}TDOA are evaluated in simulations (Section IV). Field experiments dealing with the localization of GSM base stations using a single airborne sensor are presented in Section V.

The presented method allows emitter localization with a light weight and small sensor node. Only one reception channel combined with an omni-directional antenna is needed. The requirements on the communication channel bandwidth between sensor and situation display system are small. Even if the position estimate is not determined at the sensor node but is calculated at a control station on ground, only CCF and corresponding time and position information need to be transmitted. Classic TDOA approaches require the transmission of raw signal data to a reference sensor or control station, thus having higher demands on the communication channel.

The feasibility of determining the position of an emitter using a DS^{4}TDOA is shown. The proposed DS^{4}TDOA localization is more robust to smaller SNR and outperforms the S^{4}TDOA localization in both simulations and field experiments.

References

[1] A. Amar and A. J. Weiss, "Direct geolocation of stationary wideband radio signal based on time delays and doppler shifts," in *Proc. 15th Workshop on Statistical Signal Processing*, Cardiff, Wales, Sep. 2009, pp. 101–104.

[2] K. Becker, "Target Motion Analysis (TMA)," in *Advanced Signal Processing Handbook*, S. Stergioulos, Ed. New York, NY: CRC Press, 2001, ch. 9, pp. 284–301.

[3] R. Kaune, D. Musicki, and W. Koch, "On passive emitter tracking in sensor networks," in *Sensor Fusion and its Applications*, C. Thomas, Ed. InTech, 2010, ch. 13, pp. 293–318.

[4] M. Oispuu, "Direct state determination of multiple sources with intermittent emission," in *Proc. 17th European Signal Processing Conference*, Glasgow, Scotland, Aug. 2009, pp. 1948–1952.

[5] M. Oispuu and U. Nickel, "Direct detection and position determination of multiple sources with intermittent emission," *Signal Processing*, vol. 90, pp. 3056–3064, Dec. 2010.

[6] M. Pourhomayoun and M. L. Fowler, "Distributed computation for direct position determination emitter location," *IEEE Trans. Aerosp. Electron. Syst.*, vol. 50, pp. 2878–2889, Oct. 2014.

[7] S. V. Schell and W. A. Gardner, "High-resolution direction finding," in *Handbook of Statistics, Signal Processing and its Applications*, N. K. Bose and C. R. Rao, Eds. Elsevier, 1993, vol. 10, ch. 18, pp. 755–817.

[8] C. Steffes, "Novel TDoA-based single sensor localization approach using signal structure information," in *Proc. 12th Workshop on Positioning, Navigation and Communication (WPNC)*, Dresden, Germany, Mar. 2015.

[9] S. Stein, "Algorithms for ambiguity function processing," *IEEE Trans. Acoust., Speech, Signal Processing*, vol. 29, pp. 588–599, Jun. 1981.

[10] D. J. Torrieri, "Statistical theory of passive location system," *IEEE Trans. Aerosp. Electron. Syst.*, vol. 20, pp. 183–198, Mar. 1984.

[11] A. J. Weiss, "Direct position determination of narrowband radio frequency transmitters," *IEEE Signal Processing Lett.*, vol. 11, pp. 513–516, May 2004.

[12] A. J. Weiss and A. Amar, "Direct position determination of multiple radio transmitters," in *Advances in Direction-of-Arrival Estimation*, S. Chandran, Ed. Norwood, MA: Artech House, 2006, ch. 11, pp. 213–239.